

BY JULIE D. PULLEN, ARNOLD L. GORDON,  
JANET SPRINTALL, CRAIG M. LEE, MATTHEW H. ALFORD,  
JAMES D. DOYLE, AND PAUL W. MAY

# Atmospheric and Oceanic Processes in the Vicinity of an Island Strait



**ABSTRACT.** In early February 2008, the mean flow through the Philippines' Mindoro Strait reversed. The flow was southward through the strait during late January and northward during most of February. The flow reversal coincided with the period between two Intensive Observational Period cruises (IOP-08-1 and IOP-08-2) sponsored by the Office of Naval Research as part of the Philippine Straits Dynamics Experiment (PhilEx). Employing high-resolution oceanic and atmospheric models supplemented with in situ ocean and air measurements, we detail the regional and local conditions that influenced this flow reversal. High-resolution air-sea simulations captured the flow reversal and agreed with measured currents from two moorings in the vicinity of Mindoro Strait. A short (January 24–27) easterly monsoon surge and a longer (February 9–16) northerly surge were represented in the model as well as in QuikSCAT and underway wind data taken during IOP-08-2. Mesoscale oceanic dipole eddies off Mindoro and Luzon islands were formed/enhanced and subsequently detached during these wind events. The cyclonic eddy in the dipole pair associated with the easterly surge was opportunistically sampled during the IOP-08-1 cruise, and the modeled eddy characteristics were verified using in situ shipboard data. The predominant geostrophic southward flow through the strait was interrupted by a strong and sustained wind-driven (by the northerly surge) flow reversal in early February. Enhanced upper-ocean stratification in winter 2008 due to anomalously high precipitation served to isolate the observed near-surface flow.

## INTRODUCTION

Local, regional, and remote oceanic and atmospheric conditions drive ocean circulation through the Philippine Archipelago. Here, we survey the contributions of these processes, acting on different scales, to the dynamics of a strait. Mindoro Strait (Figure 1a) is an important conduit of exchange between the archipelago's interior (Sulu Sea) and exterior (South China Sea). We aim to elucidate the various factors contributing to the flow through Mindoro Strait, so as to create an integrated picture of the mechanisms involved in a reversal of the mean current through a major pathway.

Two Office of Naval Research (ONR)-sponsored Philippine Straits Dynamics

Experiment (PhilEx) research cruises, designated Intensive Observational Period (IOP)-08-1 and IOP-08-2, plied the waters of the Philippine Archipelago during boreal winter 2008. In the period between the two cruises, the flow in Mindoro Strait reversed from southward to northward. Our work synthesizes observations and modeling to probe the role various forcing factors, including winds, eddies, and stratification, play in the evolution of the flow reversal.

## WIND JETS AND MESOSCALE DIPOLE EDDIES

As previously described in Pullen et al. (2008), monsoon surges (intensifications in the near-surface winds) lead

to the formation and detachment of a pair of mesoscale oceanic dipole eddies in the coastal waters adjacent to Mindoro and Luzon islands. The eddies move away from the coast and travel westward across the South China Sea, interacting with the complex offshore eddy field along the way. Pullen et al.

pathways of transport, and the implications for biology. They found that coastal waters near Mindoro and Luzon islands, including Manila Bay and waters near the western entrance of the Verde Island Passage, were source waters for the eddies. Waters located deeper inside the Verde Island Passage did not significantly

et al., 2000; Flament et al., 2001). In these locales, wind-driven dynamics contribute to the dipole formation via Ekman pumping (Chavanne et al., 2002; Sangrà et al., 2007). More recent research suggests that in different places in the Hawaiian Island region (Yoshida et al., 2010) either the wind or the instability mechanism dominates. Furthermore, at various times of the year in the Canary Islands (Piedeleu et al., 2009), the wind or the instability mechanism may play a stronger role in the Von Karman-like sequential shedding of counter-rotating eddies. Other processes associated with the motion of island lee eddies include self-advection of the eddy pair, advection by the background current, and westward drift via the beta effect (Cushman-Roisin et al., 1990).

During the first of the winter 2008 research cruises, we used Coupled Ocean-Atmosphere Mesoscale Prediction System (COAMPS) real-time forecasts to guide our sampling strategy. The model used 9-km resolution for the atmosphere and 3-km resolution for the ocean. In the simulations presented here, the basic configuration is the same as described in Pullen et al. (2008), but now includes tides specified at the boundaries from the Oregon State University tide

“ IN THE PERIOD BETWEEN THE TWO CRUISES, THE FLOW IN MINDORO STRAIT REVERSED FROM SOUTHWARD TO NORTHWARD. ”

(2008) used high-resolution oceanic and atmospheric modeling to document the generation and migration of these eddies in response to the atmospheric surge events. Satellite observations of sea surface temperature, winds, and chlorophyll were used to verify the wind and eddy characteristics produced by the ocean and atmosphere models. In that research, it was hypothesized that the oceanic eddies are a robust response to episodically enhanced winds (monsoon surges) arising from displacements in atmospheric pressure systems over Asia; the synoptic meteorology of monsoon surges is detailed in Chang et al. (2006) and Wu and Chan (1995, 1997).

Rypina et al. (2010) further characterized the Philippine dipole eddies of Pullen et al. (2008) from the perspective of chaotic advection—revealing the stable and unstable manifolds (special material curves that guide water dispersal over time) of the flow structures, their

contribute to eddy formation. These discoveries are further evidence of the uniquely wind-driven origin of the Philippine dipole eddies.

By contrast, in other volcanic island regions of the world (including the Hawaiian, Cabo Verde, and Canary islands), instabilities and fluctuations associated with ocean currents channeled through island straits are important in oceanic eddy generation and detachment (Lumpkin, 1998; Barton

---

**Julie D. Pullen** ([julie.pullen@stevens.edu](mailto:julie.pullen@stevens.edu)) is Director, Maritime Security Laboratory, Stevens Institute of Technology, Hoboken, NJ, USA. **Arnold L. Gordon** is Associate Director, Ocean and Climate Physics, Lamont-Doherty Earth Observatory of Columbia University, Palisades, NY, USA. **Janet Sprintall** is Research Scientist, Scripps Institution of Oceanography, University of California, San Diego, La Jolla, CA, USA. **Craig M. Lee** is Principal Oceanographer and Associate Professor, Applied Physics Laboratory, University of Washington, Seattle, WA, USA. **Matthew H. Alford** is Senior Oceanographer and Associate Professor, Applied Physics Laboratory, University of Washington, Seattle, WA, USA. **James D. Doyle** is Head, Mesoscale Modeling Section, Marine Meteorology Division, Naval Research Laboratory, Monterey, CA, USA. **Paul W. May** is Research Scientist, Computer Science Corporation, Monterey, CA, USA.



model (Egbert and Erofeeva, 2002).

The boreal winter IOP-08 cruises occurred during the northeast monsoon period in the Philippines. An easterly monsoon surge was predicted near the end of the IOP-08-1 cruise by our real-time atmospheric forecasts. Figure 1a,b compares the model-predicted wind with QuikSCAT  $\sim 25$ -km resolution winds. The atmospheric wind jets were oriented easterly, as best evidenced by the downwind portion of the jet originating between Mindoro and Panay islands (the Panay jet, cross in Figure 1b) extending westward across the northern tip of Palawan Island. The model wind orientation is in good agreement with the satellite-derived winds. In the Panay jet, easterly surge mean winds of  $12.7 \text{ m s}^{-1}$  and standard deviation of  $1.3 \text{ m s}^{-1}$  were produced in the model, with maximum winds of  $14.5 \text{ m s}^{-1}$ . This particular wind surge lasted  $\sim 3$  days, as determined by model winds exceeding the model wintertime mean ( $\sim 11 \text{ m s}^{-1}$ ) by one standard deviation ( $\sim 3 \text{ m s}^{-1}$ ), with diminished intensity intervals lasting less than 24 hours.

The real-time COAMPS ocean forecast (May et al., 2011) that we were consulting while at sea revealed a dipole eddy pair spinning up off the coasts of Mindoro and Luzon islands following the easterly wind surge. In response, we designed and commenced a ship track to sample the ocean cyclone (the southern eddy in the dipole pair). The 25-m acoustic Doppler current profiling (ADCP) shipboard measurements and model currents show a strong correspondence during January 27–31 of IOP-08-1 (Figure 2a,b). Notably, the approximately 100-km-diameter cyclonic eddy between  $13^\circ\text{N}$  and  $14^\circ\text{N}$  at  $119^\circ\text{E}$  is present

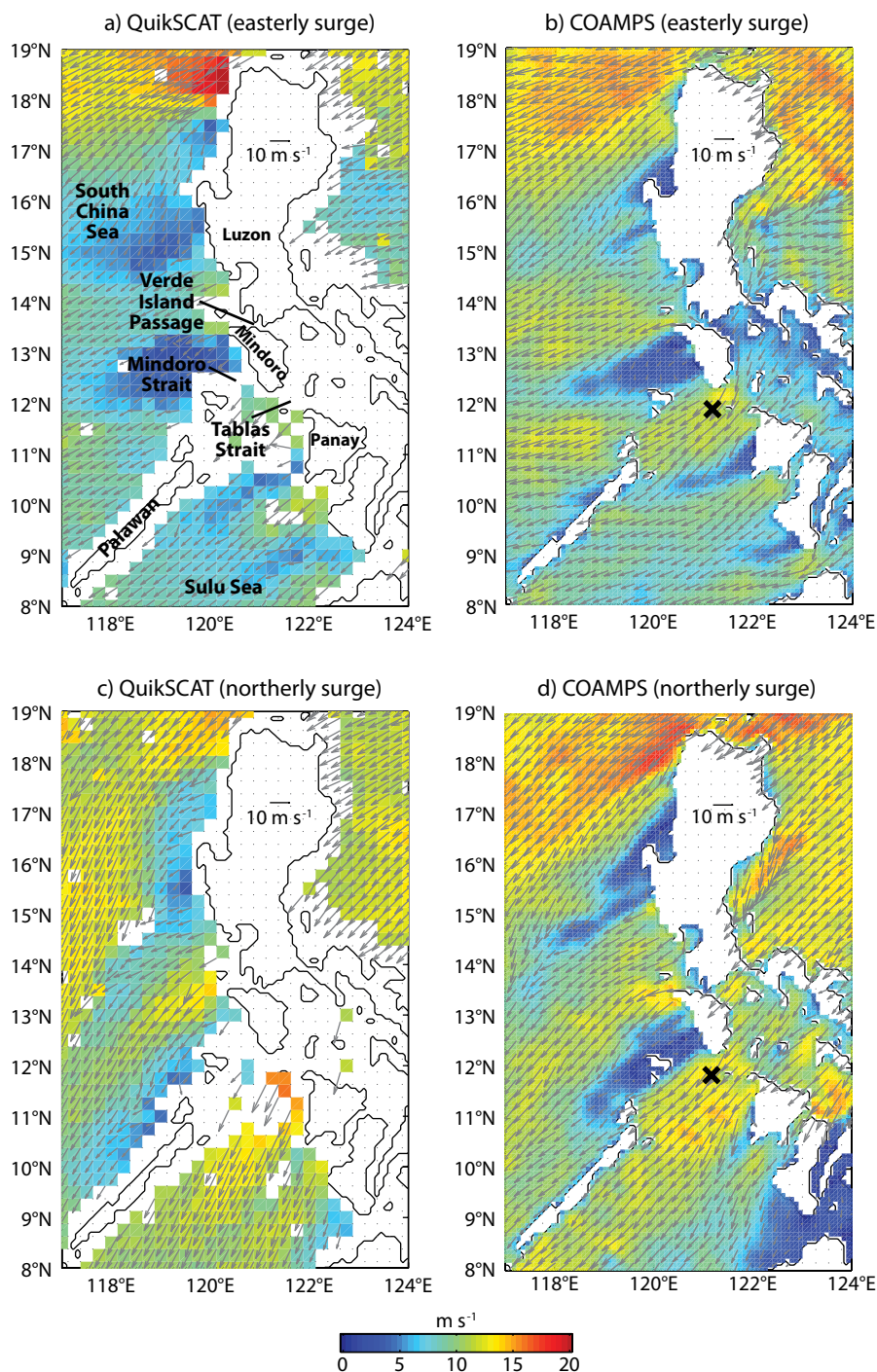


Figure 1. Near-surface winds ( $\text{m s}^{-1}$ ) from (a,c) QuikSCAT satellite (approximately 25-km resolution) and (b,d) COAMPS (Coupled Ocean-Atmosphere Mesoscale Prediction System; 9-km resolution, every third arrow shown) during two different monsoon surges in winter 2008. The top shows winds from an easterly surge at 10 UTC on January 25, 2008, while the bottom shows winds during a northerly surge that occurred at 22 UTC on February 15, 2008. The cross is located in the Panay jet (see text for statistics).

in both maps, and is apparent down to ~ 150 m in the ADCP and model fields (not shown). The southward flow (~ 25–50 cm s<sup>-1</sup>) through Mindoro Strait is also evident in both the observations and model.

The winds had calmed by the time the winter research cruise IOP-08-1 ended on January 31. About 12 days

later, the winds again intensified as part of a cold surge originating from the Asian mainland. The downwind extent of the Panay wind jet ran parallel to Palawan Island in both the model and satellite fields—thereby illustrating the northerly orientation of this particular event (Figure 1c,d). The prolonged northerly surge was longer in duration

and stronger in intensity than the earlier easterly surge. The northerly surge lasted ~ 7 days with maximum wind strength in the Panay jet of 17.1 m s<sup>-1</sup>. The mean wind speed in that location (marked by a cross in Figure 1d) over the ~ 7-day event was 12.9 m s<sup>-1</sup>, with standard deviation of 1.8 m s<sup>-1</sup>.

Figure 2c,d compares the shipboard anemometer data from the second research cruise of the northeast monsoon season (IOP-08-2) with the model-derived winds. (Unfortunately, the anemometer was not functioning properly during IOP-08-1.) Winds were enhanced in the gaps between islands and were muted and more directionally variable in the wake in the lee of Mindoro Island. The ground truthing of the predicted winds during IOP-08-2 (Figure 2c,d) and the near-surface currents during IOP-08-1 (Figure 2a,b) increases confidence in the performance of the model.

As in winter 2005 (Pullen et al., 2008), the northerly surge was somewhat stronger in the mean and had greater maximum intensity (by > 15%) than the easterly surge. The two atmospheric surge events occurring in winter 2005 were ~ 10% (1.3 m s<sup>-1</sup>) stronger in the mean than those documented here in 2008. Both easterly and northerly surge events in 2005 lasted two to three days as did the 2008 easterly surge (January 24–27, 2008), while the 2008 northerly surge lasted ~ 7 days (February 9–16, 2008) and tapered off slowly with significant wind peaks out to February 21. Fluctuation levels during the surges were similar among the events over the two years (2005 and 2008), and were quite muted (1–2 m s<sup>-1</sup>) compared to the winter seasonal standard deviation

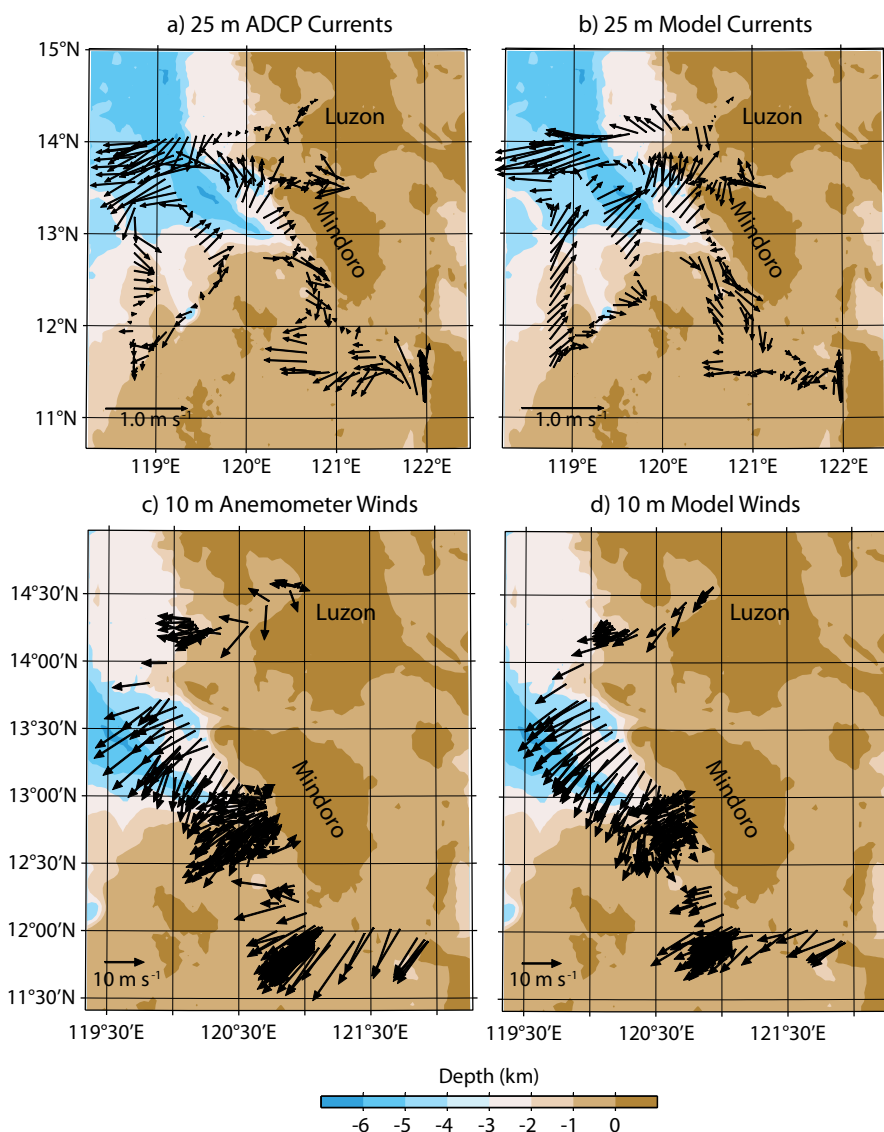
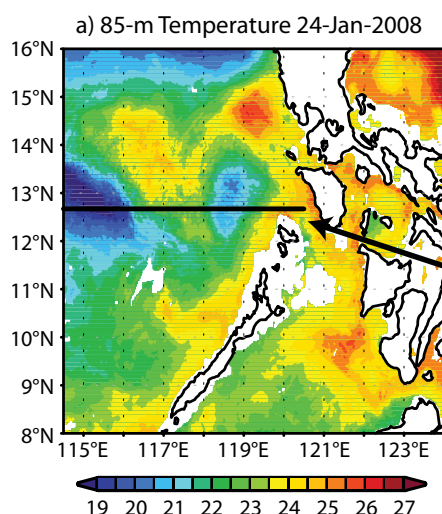


Figure 2. (a) Underway acoustic Doppler current profiler (ADCP) 25-m currents from the Intensive Observational Period (IOP)-08-1 research cruise from January 27–31, 2008, and (b) model-derived 25-m currents at the same time as they were measured. (c) Underway winds as measured by the shipboard anemometer (10-m height) during the IOP-08-2 research cruise February 10–23, and (d) model-derived 10-m winds for the corresponding sampled times.



of  $\sim 3 \text{ m s}^{-1}$ . The separation of the wind events was 17 days in 2005 and 12 days in 2008. In 2008, the easterly surge preceded the northerly surge, whereas in 2005 the sequence was reversed.

The 85-m-deep temperature derived from the model on January 24, 2008, clearly shows the northern anticyclonic (warm) eddy centered at  $119^{\circ}30'\text{E}$ ,  $15^{\circ}\text{N}$  and the southern cyclonic (cold) eddy centered at  $119^{\circ}\text{E}$ ,  $13^{\circ}\text{N}$  that are associated with the easterly surge (Figure 3a). A Hovmöller diagram constructed at latitude  $12^{\circ}40'\text{N}$  reveals the propagation of the resultant cyclonic eddies following the easterly surge and northerly surge (Figure 3b). A cyclonic eddy was present in the area before the easterly surge and was briefly perturbed by a tropical convective system that passed through the region on January 23, 2008. The oceanic cyclonic eddy strengthened and moved into the South China Sea during the easterly monsoon pulse that began the next day. Frequently, pre-existing eddies are intensified and repositioned or launched during wind events, as was also the case in the simulations of winter 2005.

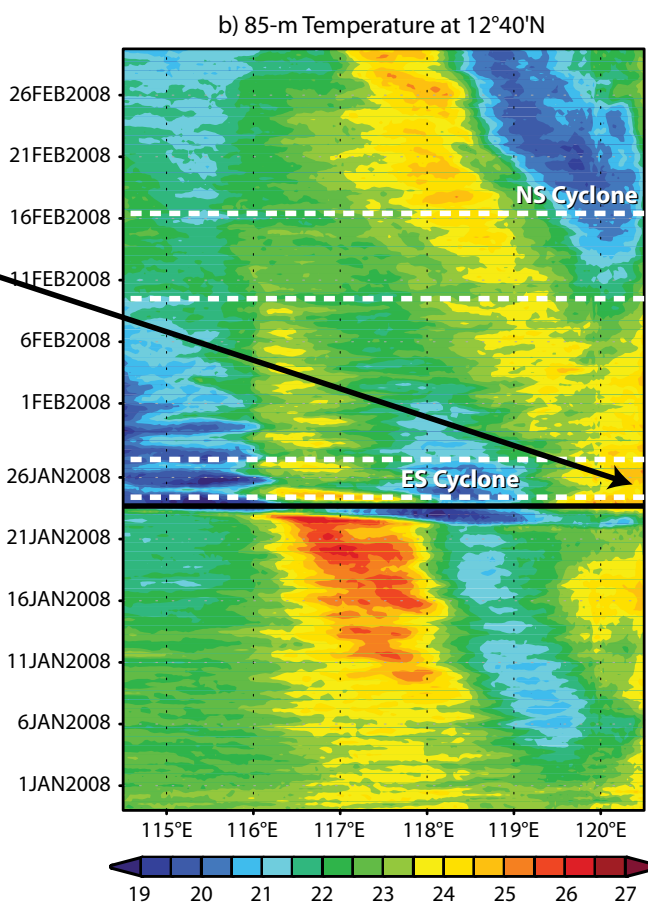


Figure 3. (a) 85-m-deep model temperature ( $^{\circ}\text{C}$ ) showing the dipole cold eddy ( $\sim 13^{\circ}\text{N}$ ) and warm eddy ( $\sim 15^{\circ}\text{N}$ ) on January 24, 2008, during the easterly monsoon surge. (b) A Hovmöller diagram of 85-m temperature at the location of the section shown in the left panel. The cyclones associated with the easterly (ES) and northerly (NS) surges are labeled, and the surge durations are denoted with the dashed white lines. The disturbance on January 23 was caused by a tropical convective system that passed through the region.

### MINDORO STRAIT FLOW REVERSAL

As part of the PhilEx program, several moorings were instrumented in the vicinity of Mindoro Strait. The Moored Profiler (MP1; Morrison et al., 2001) and Mindoro mooring velocity measurements captured the flow reversal in Mindoro Strait and give more details as to how the reversal evolved over time. At the end of the easterly surge, the 25-m currents were directed to the south over a several week period at the MP1 site in both the model and observations (Figure 4a). The model produced a stronger current than was observed. The mean observed current in the interval between surges is  $-7 \text{ cm s}^{-1}$ , while the model produced a mean current of  $-27 \text{ cm s}^{-1}$ . The southward flow did

not occupy the strait's full width in the January 30 model results (Figure 4b). Indeed, a local anticyclonic eddy was situated within the strait in the velocity maps from January 30, 2008, (Figure 4b) and February 1 (Figure 4c). The transient local anticyclonic eddy in Mindoro Strait is an intermittent flow feature that occurs when winds are relatively weak (Figure 4c). The intensity and shape of the small anticyclonic eddy appeared to vary over time, and this variability may be a factor in the model-to-observation along-strait mean current discrepancy.

As the northerly surge commenced, the current at MP1 reversed to northward and increased dramatically. The mean velocity measured at the MP1 site was  $50 \text{ cm s}^{-1}$  during February 10–22, while the modeled current was quite a



bit weaker at  $9 \text{ cm s}^{-1}$ . MP1 was located on the periphery of a strong northward jet in the model (Figure 4d), and positional variations may influence the model-to-observation agreement. The standard deviation of the 25-m current at MP1 for the time period February 10–22 was  $16 \text{ cm s}^{-1}$  in the observations and

$11 \text{ cm s}^{-1}$  in the model, so the fluctuation structure was reproduced reasonably well in the model. To verify that modeled ocean jet speeds attained the levels seen in the observation, a model location  $\sim 20 \text{ km}$  west of the actual MP1 site was chosen (Figure 4a, blue line). The close correspondence between the

model at this displaced site (mean of  $49 \text{ cm s}^{-1}$  during February 10–22) and the observation (mean of  $50 \text{ cm s}^{-1}$  during February 10–22) reinforces the conclusion that the position of the core of the modeled jet was slightly displaced relative to that of the observed jet during this time.

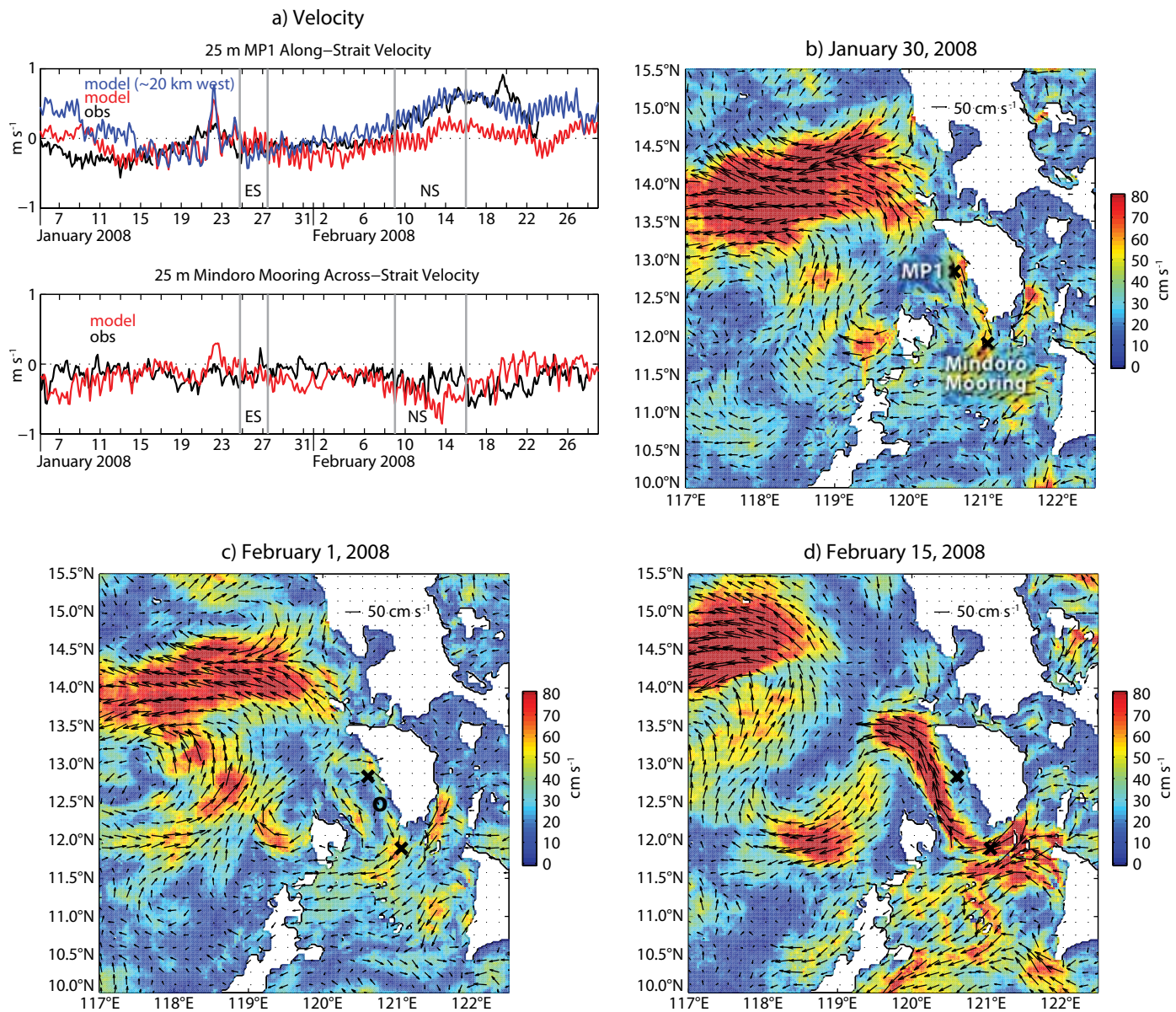


Figure 4. (a) Measured and modeled 25-m currents at two moorings: MP1 and the Mindoro mooring, whose locations are marked with crosses. The other panels show snapshots of the model-produced surface current field (3-km resolution, every sixth arrow shown) on (b) January 30, (c) February 1, and (d) February 15, 2008. In panel (a), currents are rotated  $-45^\circ$  to create along- and across-strait velocities. The “O” in panel (c) denotes the core of the small anticyclonic eddy within Mindoro Strait.

At the Mindoro mooring, intensified cross-strait flow occurred following the northerly monsoon surge. This flow was  $-32$  ( $-51$ )  $\text{cm s}^{-1}$  on average during February 10–22 in the observation (model). As depicted in the model-derived surface current map for February 15 (Figure 4d), this flow was part of a continuous westward current emerging from Tablas Strait between Panay and Mindoro islands.

In our prior simulations of winter 2005, the Mindoro Strait flow was southward in the period encompassing the surge events (Pullen et al., 2008)—consistent with seasonal model-derived maps of Mindoro Strait that show flow is typically southward during wintertime (Han et al., 2009). This flow direction suggests a dominant geostrophic balance that was disrupted during the sustained northerly surge of February 2008 as the Mindoro Strait flow reversed to northward. An examination of model sea surface height maps (not shown) reveals a cross-strait pressure gradient that is enhanced during surge events when sea level setup develops around Palawan Island. The near-surface Ekman flow (directed to the right of the applied wind stress) presumably intensified with the onset of the prolonged northerly surge and dominated the dynamics in the vicinity of Mindoro Strait, leading to a strong northward flow through the strait.

The subsurface flow measured at the MP1 site in 2008 revealed that flow reversal extended to approximately 100 m, and was strongly surface-intensified in the upper 25–50 m (not shown). The model did not replicate the observed pronounced near-surface intensification but did better reproducing the observed attenuated currents

below 100–200 m. We explore the source of this model-to-observation discrepancy by considering the stratification.

### REGIONAL STRATIFICATION EFFECTS

In order to examine the vertical ocean structure and assess the model-to-observation correspondence, we calculate Brunt-Vaisala frequency ( $N^2$ ) and

shear  $(dU/dz)^2$  difference is greatest near the surface, with the observations displaying enhanced shear relative to the model (Figure 5c,d). However, deeper in the water column the model showed characteristics more aligned with the observations.

Missing buoyancy effects may explain why the model is not sufficiently stratified near the surface, in contrast with the

“HIGH-RESOLUTION OCEANIC AND ATMOSPHERIC MODELING COMPLETES THE INTEGRATED PICTURE BY PROVIDING INSIGHT INTO THE CIRCULATION CHARACTERISTICS THAT EXIST AWAY FROM MEASUREMENT SITES.”

vertical velocity shear  $(dU/dz)^2$ , the components of gradient Richardson number  $(N^2/(dU/dz)^2)$ . The constituent in situ values come from IOP-08-1 conductivity, temperature, depth (CTD) profiles at 2-m vertical spacing, and lowered ADCP horizontal velocity at coincident sites with vertical spacing of 10 m. The model fields were produced on a vertically stretched grid with vertical spacing ranging from 2–5 m in the upper 25 m. Figure 5 displays the differenced (observed-model) near-surface quantities. Generally, in the vicinity of Mindoro Strait, the model was too well mixed as evidenced by the too weak  $N^2$  values (Figure 5a). However, the model-observation correspondence increased with depth at a representative station (Figure 5b). Likewise, in Mindoro Strait, the square of the vertical

numerous station observations. Indeed, upper ocean stratification was enhanced in winter 2008 due to anomalously high precipitation probably related to the La Niña event that peaked in February 2008. Interestingly, winter 2008 was the rainiest on record in 40 years (Gordon et al., 2011). Precipitation effects were underrepresented in the model due to the absence of river runoff in the simulations coupled with the difficulty numerical weather models have in accurately simulating local-area rainfall. The impact of river runoff is evident in the spatial pattern of near-surface  $N^2$  differences (Figure 5a). The observed  $N^2$  is higher for coastal locations (Mindoro, Verde Island Passage, Panay), while model  $N^2$  is higher for outer (offshore) Mindoro sites and the Panay stations during the second occupation (blue circles). Buoyant



discharge not captured by the model is most prevalent right near the coast, leading to larger observed  $N^2$  values in those locations. The buoyancy input due to the freshwater created a more layered near-surface flow in the observations.

## CONCLUSIONS

We brought together ocean and atmosphere model results and observations in order to examine the evolution of a flow reversal in Mindoro Strait. The flow reversal took place between two

intensive sampling research cruises: southward flow was measured during IOP-08-1 while northward flow was encountered during IOP-08-2. In situ measurements, including mooring and CTD data, complement the underway and satellite data to form a picture of the conditions and timing of the flow transition. High-resolution oceanic and atmospheric modeling completes the integrated picture by providing insight into the circulation characteristics that exist away from measurement sites.

Wind jets play a primary role in shaping the flow by spinning up dipole eddies in the lee of Mindoro and Luzon islands via Ekman pumping. We were fortunate to sample within a cyclonic eddy using shipboard measurements following an easterly surge in January 2008. Basic features of the eddy, including size ( $\sim 100$  km), current magnitude ( $25\text{--}50$  cm  $s^{-1}$ ), and depth ( $\sim 150$  m), in the model largely agreed with underway ADCP observations.

The sea level setup against Palawan Island caused by the wintertime surface winds creates a geostrophic flow that is predominantly southward through Mindoro Strait. In the particular flow reversal studied here the prolonged northerly surge lasted over a week—at least twice as long as the prior easterly surge. This uncharacteristically long northerly surge facilitated a directly wind-forced northward Ekman drift through Mindoro Strait.

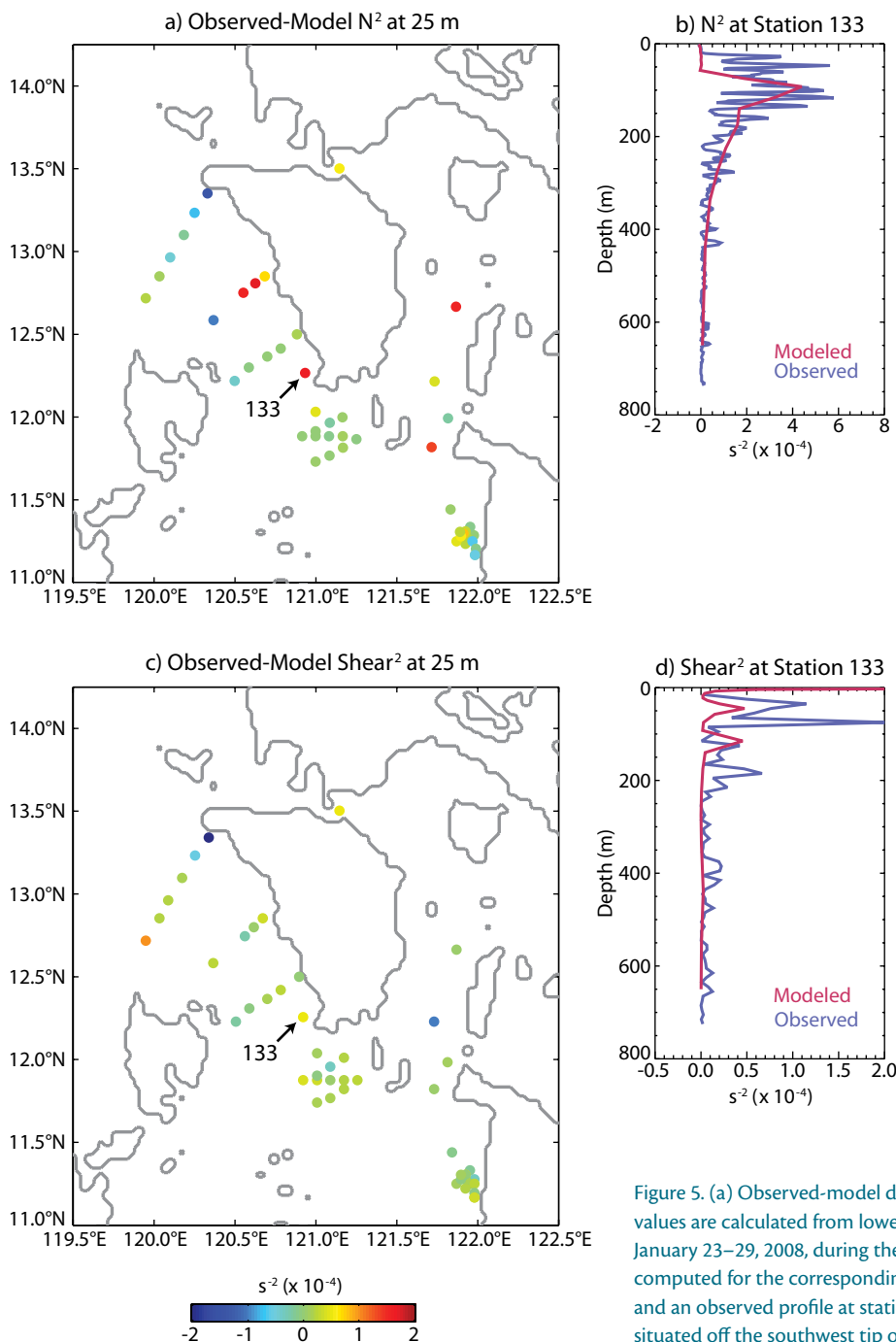



Figure 5. (a) Observed-model difference plots of 25-m  $N^2$  (c) and shear<sup>2</sup>. The observed values are calculated from lowered ADCP and CTD data at 48 stations occupied January 23–29, 2008, during the IOP-08-1 research cruise. The model values are computed for the corresponding times and locations. In the other panels, a modeled and an observed profile at station 133 of (b)  $N^2$  and (d) shear<sup>2</sup> are shown. Station 133, situated off the southwest tip of Mindoro Island, is labeled in the left panels.

A contributing factor in the strong ocean response to the wind stress was the anomalously fresh near-surface waters that were sampled by the research cruises in winter 2008. The Philippines experienced the rainiest winter in 40 years in 2008, and this freshwater lens created more stratified flow in many parts of the archipelago. Although the modeled wind and current fields were in reasonable agreement with many observed quantities, the model produced an upper ocean structure that was not sufficiently stratified. The model configuration did not account for river runoff nor accurately predict local rainfall. Future simulations will include river discharge and improved microphysical parameterizations.

The dominance of wind-driven processes is a hallmark of the Philippine region. The compounding ways that winds can act on ocean structures such as eddies to both move them around and induce local flows, as demonstrated here, is beginning to receive more attention in process studies (Morel and Thomas, 2009). The complex Philippine straits are fascinating realistic examples where island geometry renders channel and gap flow highly dynamic in both the ocean and the atmosphere.

## ACKNOWLEDGEMENTS

We are grateful to Pierre Flament for valuable discussions. COAMPS is a registered trademark of the Naval Research Laboratory. The research support for J. Pullen was provided by a Marie Tharp visiting fellowship at the Earth Institute, Columbia University, as well as Office of Naval Research (ONR) program element 0601153N and grant N00014-10-1-0300. A.L. Gordon was funded by ONR grant N00014-09-1-0582

and this is Lamont-Doherty Earth Observatory contribution number 7430. J. Sprintall was funded by ONR grant N00014-06-1-0690. J. Doyle and P. May were supported by the Office of Naval Research (ONR) program element 0601153N. Thanks to the crew of R/V *Melville* for their assistance. 

## REFERENCES

- Barton, E.D., G. Basterretxea, P. Flament, E.G. Mitchelson-Jacob, B. Jones, J. Aristegui, and F. Herrera. 2000. Lee region of Gran Canaria. *Journal of Geophysical Research* 105(C7):17,173–17,193.
- Chang, C.-P., Z. Wang, and H. Hendon. 2006. The Asian winter monsoon. Pp. 89–127 in *The Asian Monsoon*. B. Wang, ed., Springer, Berlin.
- Chavanne, C., P. Flament, R. Lumpkin, B. Dousset, and A. Bentamy. 2002. Scatterometer observations of wind variations induced by oceanic islands: Implications for wind-driven ocean circulation. *Canadian Journal of Remote Sensing* 28(3):466–474.
- Cushman-Roisin, B., E.P. Chassignet, and B. Tang. 1990. Westward motion of mesoscale eddies. *Journal of Physical Oceanography* 20:758–768.
- Egbert, G.D., and S.Y. Erofeeva. 2002. Efficient inverse modeling of barotropic ocean tides. *Journal of Atmospheric and Oceanic Technology* 19:183–204.
- Flament, P., R. Lumpkin, J. Tournadre, and L. Armi. 2001. Vortex pairing in an unstable anticyclonic shear flow: Discrete subharmonics of one pendulum day. *Journal of Fluid Mechanics* 440:401–409.
- Gordon, A.L., J. Sprintall, and A. Ffield. 2011. Regional oceanography of the Philippine Archipelago. *Oceanography* 24(1):14–27.
- Han, W., A.M. Moore, J. Levin, B. Zhang, H.G. Arango, E. Curchitser, E. DiLorenzo, A.L. Gordon, and J. Lin. 2009. Seasonal surface ocean circulation and dynamics in the Philippine Archipelago region during 2004–2008. *Dynamics of Atmospheres and Oceans*, doi:10.1016/j.dynatmoce.2008.10.007.
- Lumpkin, C.F. 1998. Eddies and currents of the Hawaiian Islands. PhD Thesis, University of Hawaii, 281 pp.
- May, P.W., J.D. Doyle, J.D. Pullen, and L.T. David. 2011. Two-way coupled atmosphere-ocean modeling of the PhilEx Intensive Observational Periods. *Oceanography* 24(1):48–57.
- Morel, Y., and L.N. Thomas. 2009. Ekman drift and vortical structures. *Ocean Modelling* 27:185–197.
- Morrison, A.T., J.D. Billings, K.W. Doherty, and J.M. Toole. 2001. The McLane Moored Profiler: A platform for physical, biological, and chemical oceanographic measurements. Paper presented at the Oceanology International 2000 Conference, Brighton, UK.
- Piedeleu, M., P. Sangrà, A. Sanchez-Vidal, J. Fabres, C. Gordo, and A. Calafat. 2009. An observational study of oceanic eddy generation mechanisms by tall deep-water islands (Gran Canaria). *Geophysical Research Letters* 36, L14605, doi:10.1029/2008GL037010.
- Pullen, J., J.D. Doyle, P. May, C. Chavanne, P. Flament, and R.A. Arnone. 2008. Monsoon surges trigger oceanic eddy formation and propagation in the lee of the Philippine Islands. *Geophysical Research Letters* 35, L07604, doi:10.1029/2007GL033109.
- Rypina, I.I., L.J. Pratt, J. Pullen, J. Levin, and A.L. Gordon. 2010. Chaotic advection in an archipelago. *Journal of Physical Oceanography* 40:1,988–2,006, doi:10.1175/2010JPO4336.1.
- Sangrà, P., M. Auladell, A. Marrero-Díaz, J.L. Pelegrí, E. Fraile-Nuez, A. Rodríguez-Santana, J.M. Martín, E. Mason, and A. Hernández-Guerra. 2007. On the nature of oceanic eddies shed by the Island of Gran Canaria. *Deep-Sea Research Part I* 54:687–709.
- Wu, M.C., and J.C.L. Chan. 1995. Surface features of winter monsoon surges over South China. *Monthly Weather Review* 123:662–680.
- Wu, M.C., and J.C.L. Chan. 1997. Upper-level features associated with winter monsoon surges over South China. *Monthly Weather Review* 125:317–340.
- Yoshida, S., B. Qiu, and P. Hacker. 2010. Wind-generated eddy characteristics in the lee of the island of Hawaii. *Journal of Geophysical Research* 115, C03019, doi:10.1029/2010JC005417.